Stem Cell Reports, Volume *12*

Supplemental Information

Involvement of p38 in Age-Related Decline in Adult Neurogenesis via Modulation of Wnt Signaling

Yoshitaka Kase, Kinya Otsu, Takuya Shimazaki, and Hideyuki Okano

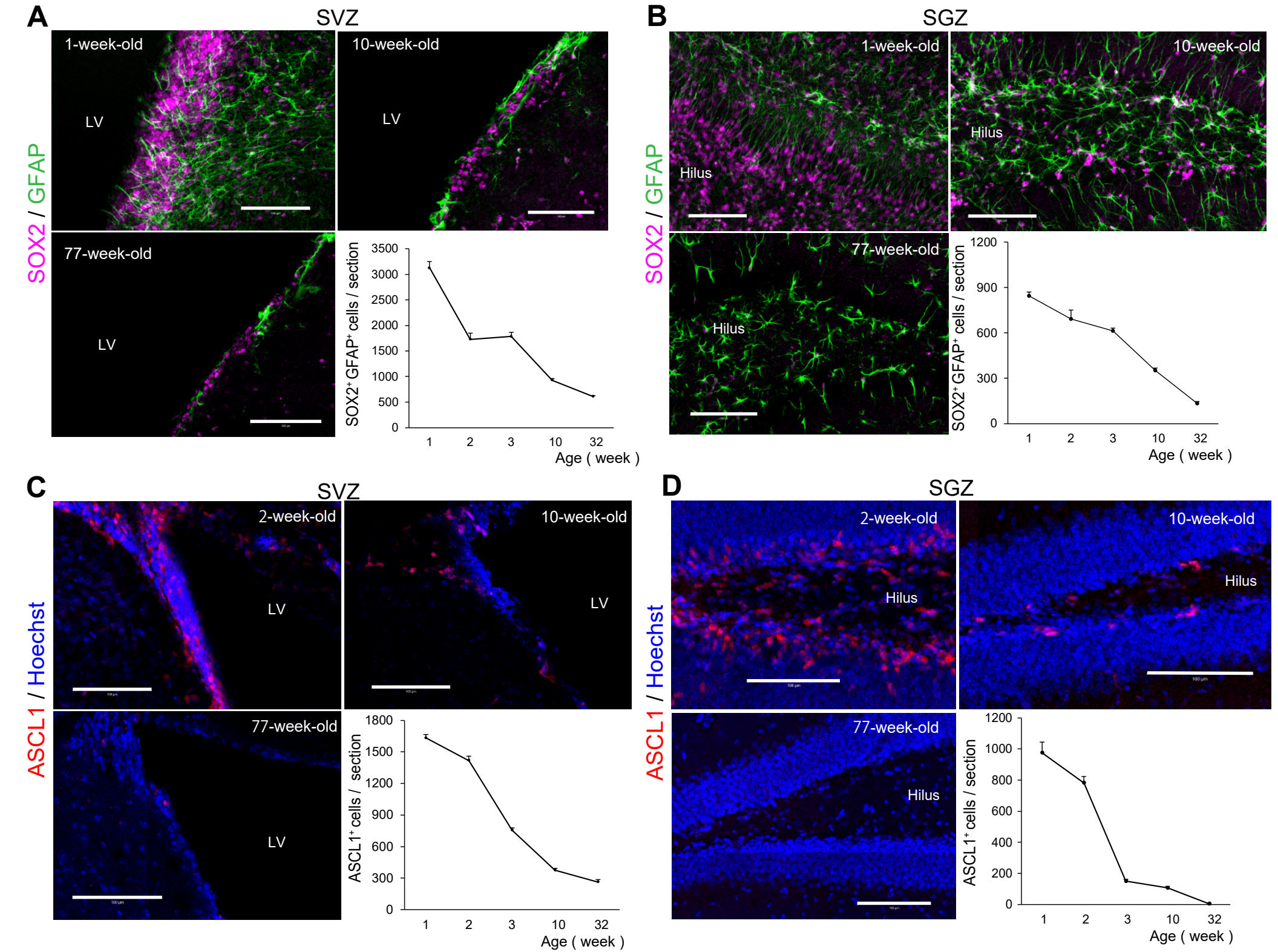
A
SVZ
1-week-old
10-week-old
77-week-old
LV
SOX2 / GFAP
SOX2⁺ GFAP⁺ cells / section
Age (week)
B
SGZ
Hilus
C
ASCL1 / Hoechst
2-week-old
ASCL1⁺ cells / section
D

Figure S1

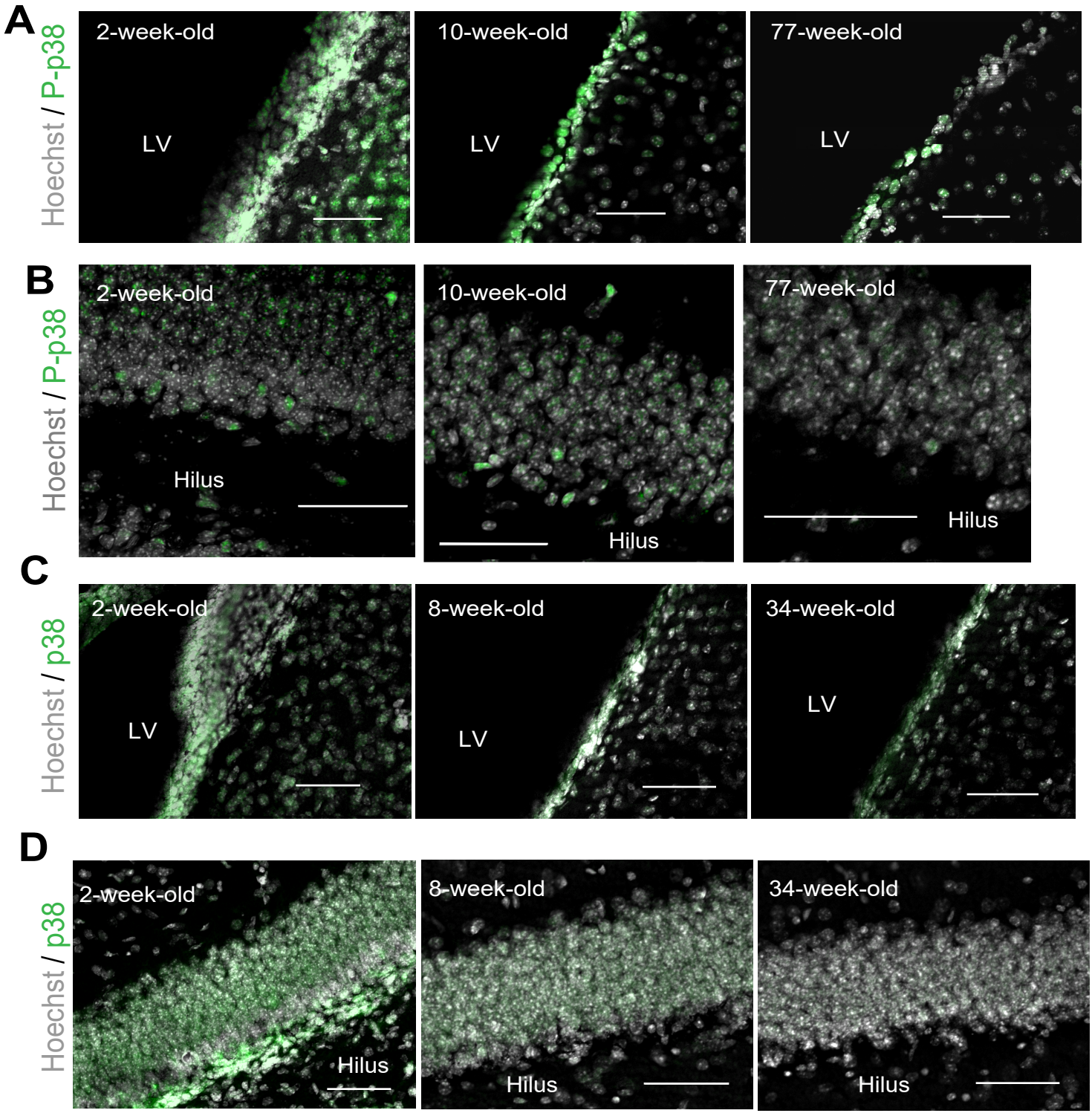
A
Hoechst / P-p38
2-week-old
LV
10-week-old
LV
77-week-old
LV
B
Hoechst / P-p38
2-week-old
Hilus
10-week-old
Hilus
77-week-old
Hilus
C
Hoechst / p38
2-week-old
LV
8-week-old
LV
34-week-old
LV
D
Hoechst / p38
2-week-old
Hilus
8-week-old
Hilus
34-week-old
Hilus

Figure S2

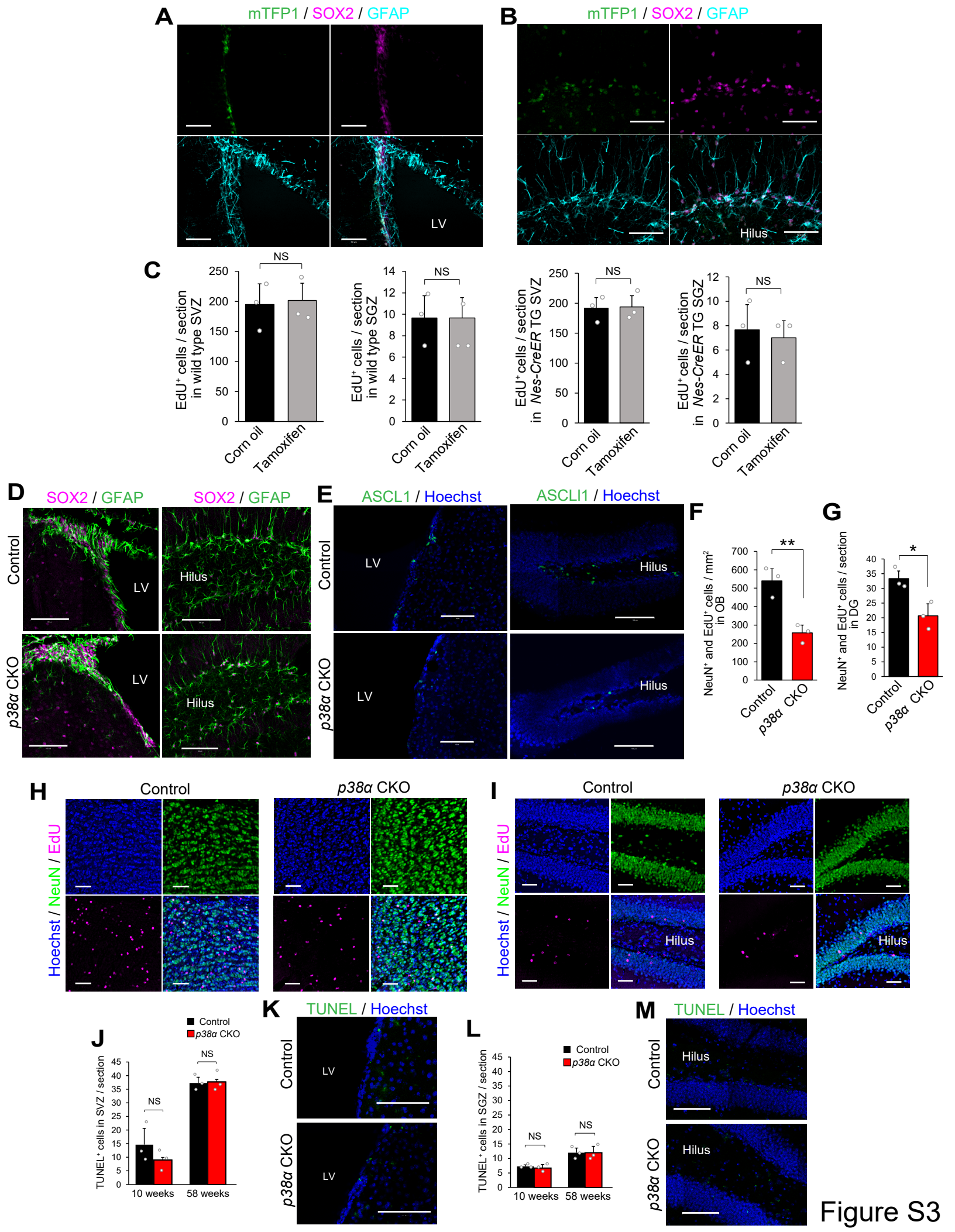
A
mTFP1 / SOX2 / GFAP
LV
B
mTFP1 / SOX2 / GFAP
Hilus
C
NS
EdU+ cells / section in wild type SVZ
EdU+ cells / section in wild type SGZ
EdU+ cells / section in Nes-CreER TG SVZ
EdU+ cells / section in Nes-CreER TG SGZ
Corn oil
Tamoxifen
D
SOX2 / GFAP
SOX2 / GFAP
Control
p38α CKO
LV
Hilus
E
ASCL1 / Hoechst
ASCLI1 / Hoechst
Control
p38α CKO
LV
Hilus
F
**
NeuN+ and EdU+ cells / mm2 in OB
Control
p38α CKO
G
*
NeuN+ and EdU+ cells / section in DG
Control
p38α CKO
H
Control
p38α CKO
Hoechst / NeuN / EdU
I
Control
p38α CKO
Hoechst / NeuN / EdU
Hilus
J
Control
p38α CKO
NS
TUNEL+ cells in SVZ / section
10 weeks
58 weeks
K
TUNEL / Hoechst
Control
p38α CKO
LV
L
Control
p38α CKO
NS
TUNEL+ cells in SGZ / section
10 weeks
58 weeks
M
TUNEL / Hoechst
Control
p38α CKO
Hilus

Figure S3

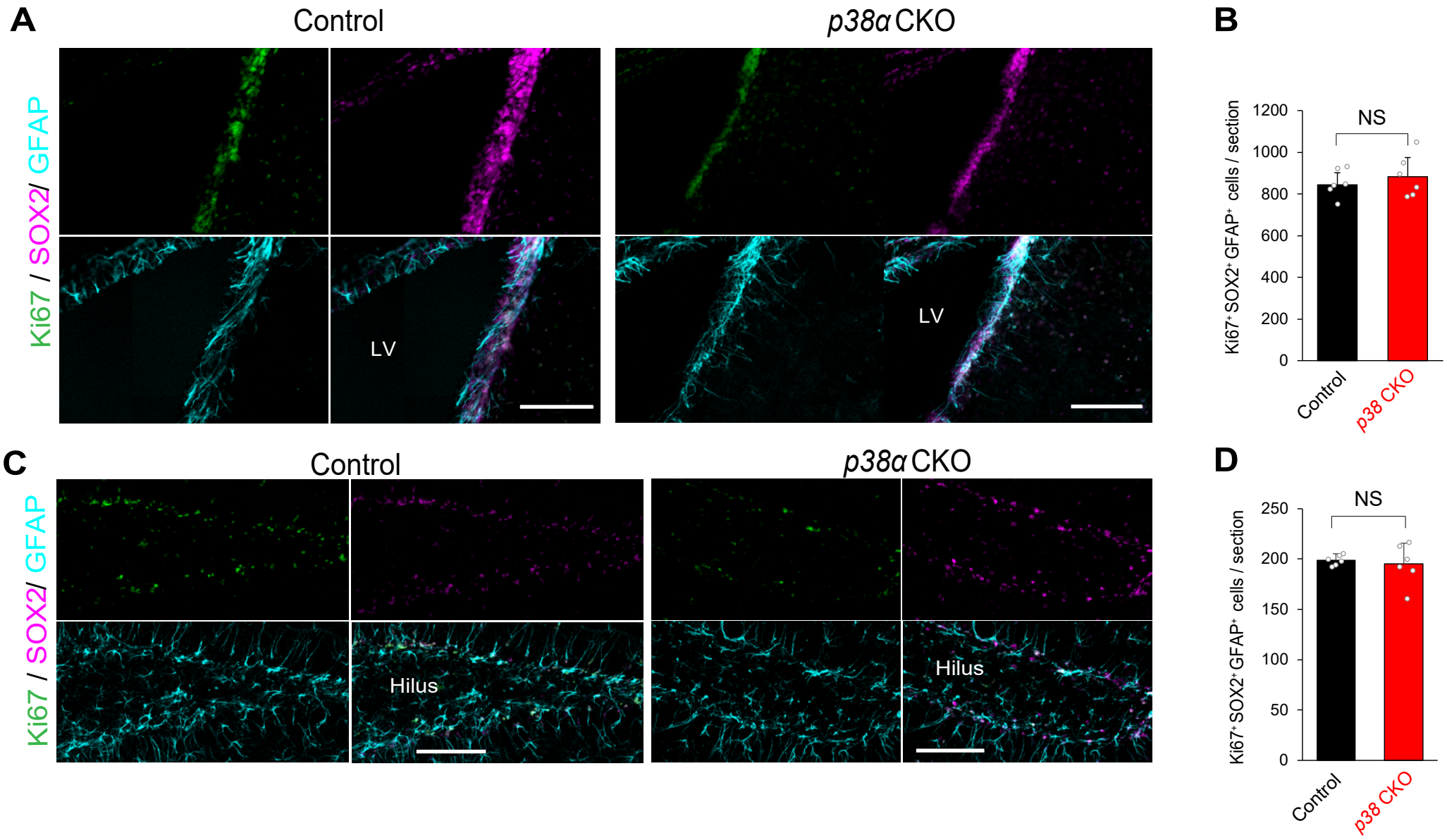
A
Control
p38α CKO
Ki67 / SOX2/ GFAP
LV
LV
B
Ki67+ SOX2+ GFAP+ cells / section
1200
1000
800
600
400
200
0
NS
Control
p38 CKO
C
Control
p38α CKO
Ki67 / SOX2/ GFAP
Hilus
Hilus
D
Ki67+ SOX2+ GFAP+ cells / section
250
200
150
100
50
0
NS
Control
p38 CKO

Figure S4

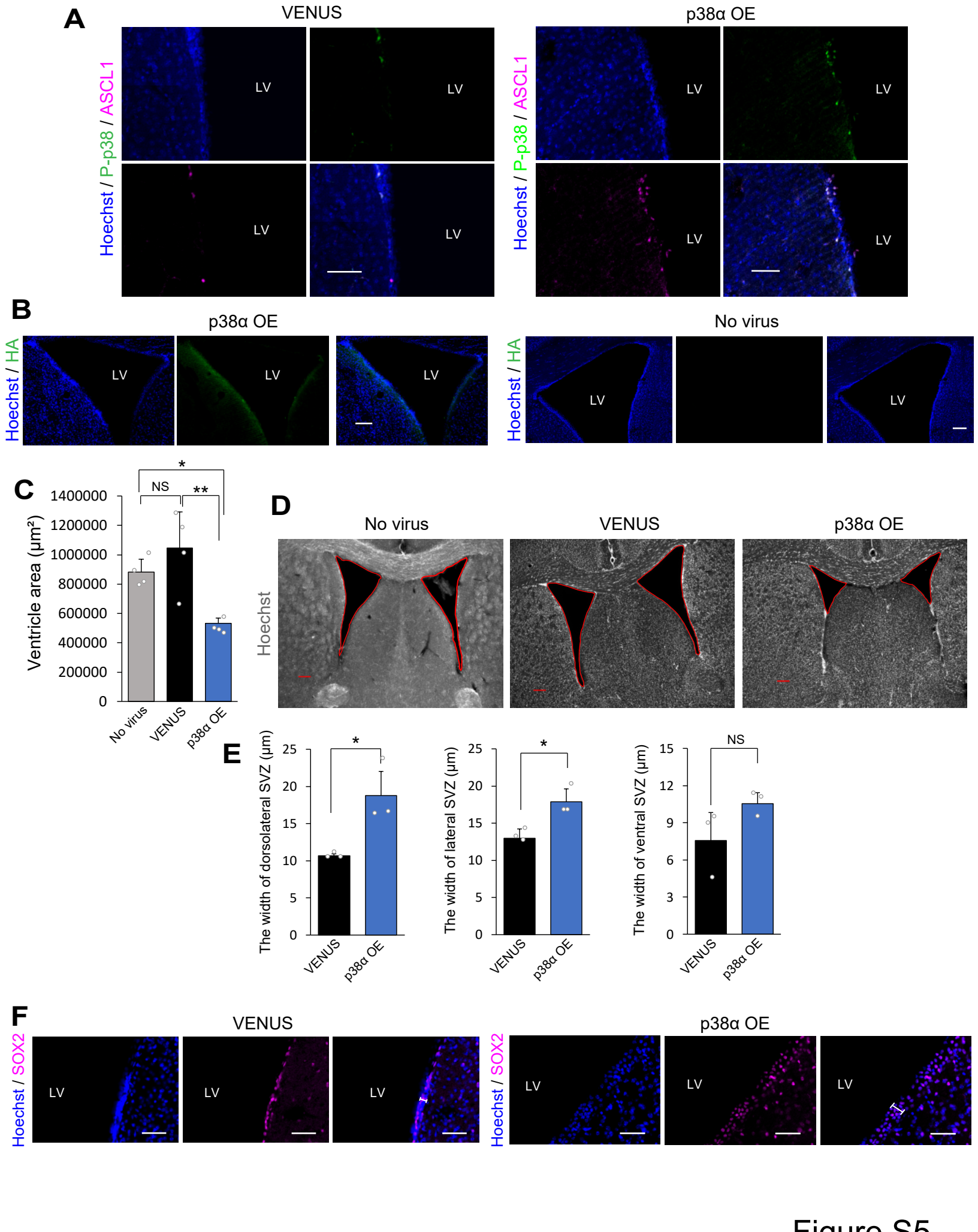
A
VENUS
p38α OE
Hoechst / P-p38 / ASCL1
LV
B
p38α OE
No virus
Hoechst / HA
C
Ventricle area (μm²)
1400000
1200000
1000000
800000
600000
400000
200000
0
NS
*
**
No virus
VENUS
p38α OE
D
No virus
VENUS
p38α OE
Hoechst
E
The width of dorsolateral SVZ (μm)
The width of lateral SVZ (μm)
The width of ventral SVZ (μm)
25
20
15
10
5
0
15
12
9
6
3
NS
VENUS
p38α OE
F
VENUS
p38α OE
Hoechst / SOX2

Figure S5

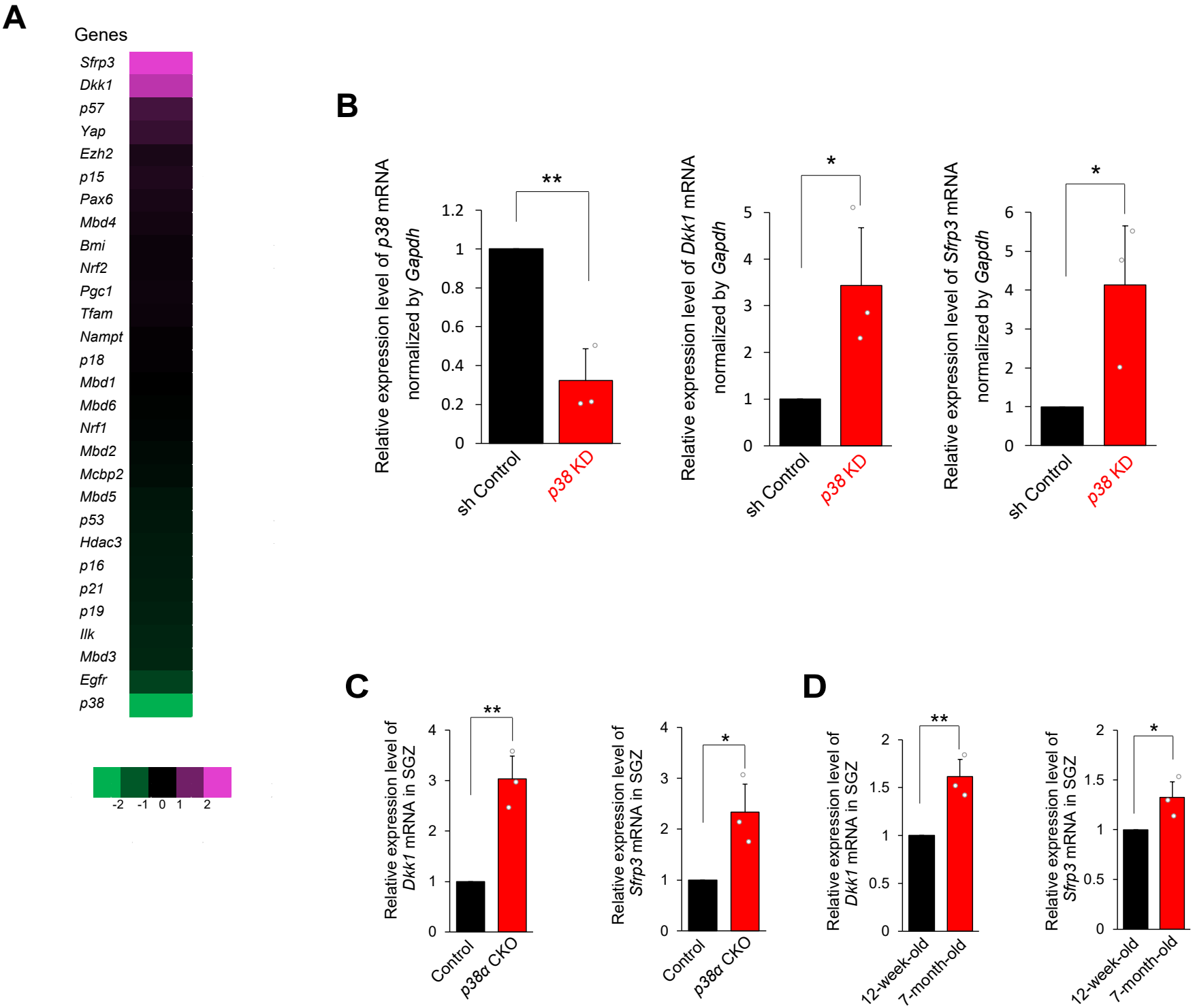
A
Genes
Sfrp3
Dkk1
p57
Yap
Ezh2
p15
Pax6
Mbd4
Bmi
Nrf2
Pgc1
Tfam
Nampt
p18
Mbd1
Mbd6
Nrf1
Mbd2
Mcbp2
Mbd5
p53
Hdac3
p16
p21
p19
Ilk
Mbd3
Egfr
p38
-2 -1 0 1 2
B
Relative expression level of p38 mRNA normalized by Gapdh
**
1.2
1
0.8
0.6
0.4
0.2
0
sh Control
p38 KD
Relative expression level of Dkk1 mRNA normalized by Gapdh
*
5
4
3
2
1
0
sh Control
p38 KD
Relative expression level of Sfrp3 mRNA normalized by Gapdh
*
6
5
4
3
2
1
0
sh Control
p38 KD
C
Relative expression level of Dkk1 mRNA in SGZ
**
4
3
2
1
0
Control
p38α CKO
Relative expression level of Sfrp3 mRNA in SGZ
*
4
3
2
1
0
Control
p38α CKO
D
Relative expression level of Dkk1 mRNA in SGZ
**
2
1.5
1
0.5
0
12-week-old
7-month-old
Relative expression level of Sfrp3 mRNA in SGZ
*
2
1.5
1
0.5
0
12-week-old
7-month-old

Figure S6

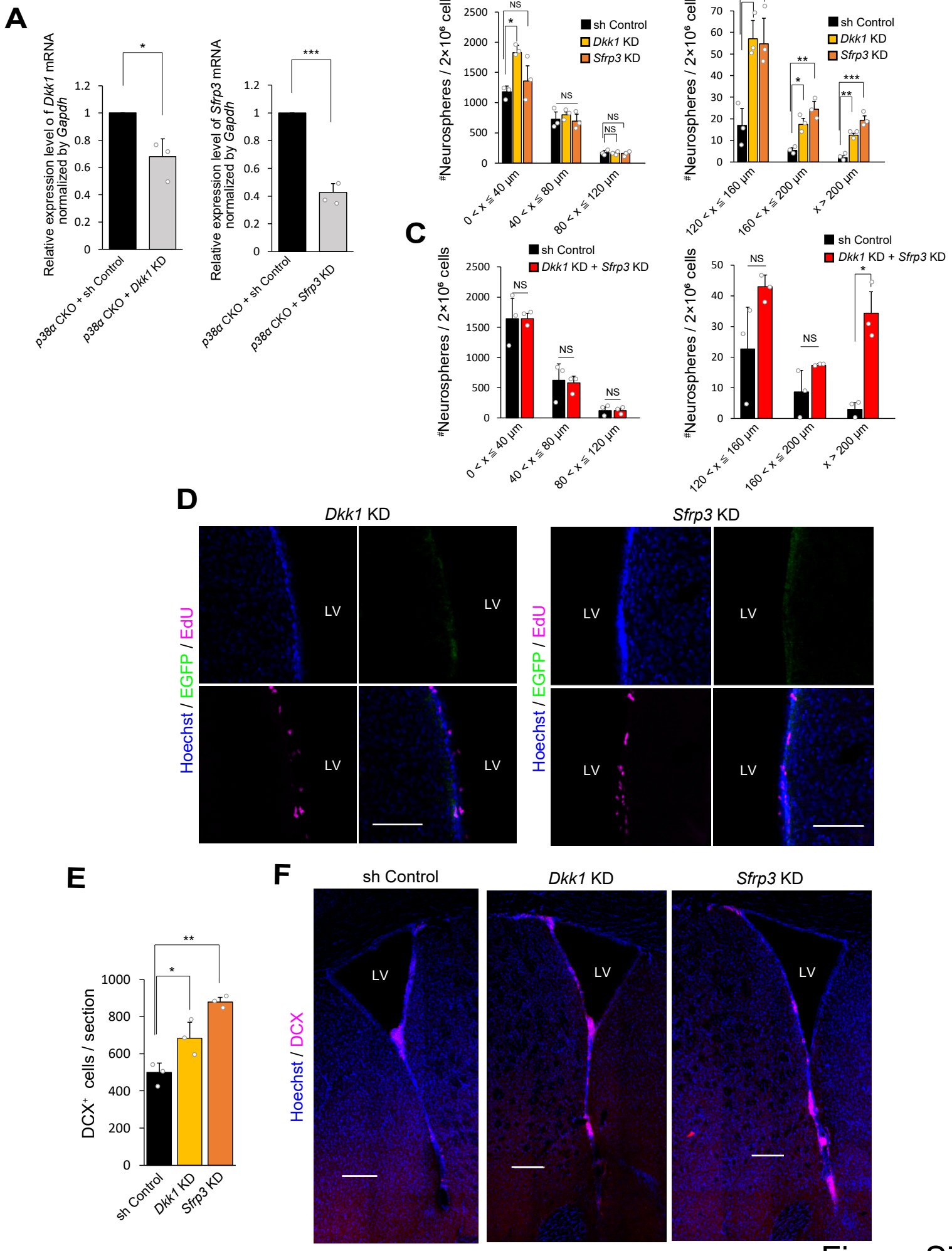
A
Relative expression level of Dkk1 mRNA normalized by Gapdh
p38α CKO + sh Control
p38α CKO + Dkk1 KD
Relative expression level of Sfrp3 mRNA normalized by Gapdh
p38α CKO + sh Control
p38α CKO + Sfrp3 KD
B
#Neurospheres / 2×10⁶ cells
sh Control
Dkk1 KD
Sfrp3 KD
0 < x ≦ 40 μm
40 < x ≦ 80 μm
80 < x ≦ 120 μm
120 < x ≦ 160 μm
160 < x ≦ 200 μm
x > 200 μm
C
#Neurospheres / 2×10⁶ cells
sh Control
Dkk1 KD + Sfrp3 KD
D
Dkk1 KD
Sfrp3 KD
Hoechst / EGFP / EdU
LV
E
DCX⁺ cells / section
sh Control
Dkk1 KD
Sfrp3 KD
F
sh Control
Dkk1 KD
Sfrp3 KD
Hoechst / DCX
LV

Figure S7

Supplemental Figure Legends

Figure S1. Decrease in NSCs and TACs During Aging, Related to Figure 1

(A and B) Age-dependent decrease in SOX2 and GFAP double-positive (+) NSCs in the SVZ and SGZ. The numbers of $SOX2^+$ (magenta)/$GFAP^+$ (green) cells in the SVZ (A) and SGZ (B) of 1-, 10- and 77-week-old mice per section were counted via confocal imaging.

(C and D) Age-dependent decrease in $ASCL1^+$ TACs (red). The numbers of $ASCL1^+$ cells in the SVZ (C) and SGZ (D) at various ages were counted as described above.

Nuclei were counterstained with Hoechst (blue). Scale bars: 100 μm.

Values in the line graphs represent the mean ± SD (*n* = 3 mice). LV: Lateral ventricle.

Figure S2. P-p38 Expression levels in NSCs and TACs Decrease with Aging, Related to Figure 1

(A and B) Representative confocal images of the SVZ (A) and SGZ (B) from 2-, 10-, and 77-week-old mice, stained with anti-phospho-p38 antibody (green) and Hoechst 33258 (gray).

(C and D) Representative confocal images of the SVZ (C) and SGZ (D) from 2, 8, and 34-week-old mice, stained with anti-p38 antibody (green) and Hoechst 33258 (gray).

Nuclei were stained with Hoechst (blue). LV: Lateral ventricle. Scale bars: 50 μm.

Figure S3. Proliferation of TACs is Specifically Impaired in *p38α* CKO Mice, Related to Figure 2

(A and B) Tamoxifen (TAM) injection into $p38\alpha^{flox/flox}$; *Nes-CreER*; $ROSA26^{CAG\text{-}mTFP1}$ mice induced bright monomeric Teal Fluorescent Protein (mTFP1) expression (green) in $SOX2^+$ (magenta)/$GFAP^+$ (cyan) NSCs in the SVZ (A) and SGZ (B). Scale bars: 50 μm.

(C) The Number of EdU^+ proliferating cells in SVZ and SGZ of wild-type and *Nes-CreER* mice which were injected with corn oil or TAM (75 mg/kg) were counted to test its toxicity. TAM and EdU administrations into mice and subsequent histochemical analyses were performed as

described in Figure 2A. There was no significant change in the number of EdU^+ cells by the TAM administration either in wild-type or *Nes-CreER* mice (*n* = 3 mice).

(D) Immunohistochemical analyses of $SOX2^+$(magenta)/$GFAP^+$(green) NSCs in the SVZ and SGZ of control and *p38α* CKO mice. Scale bars: 100 μm.

(E) Immunohistochemical analyses of $ASCL1^+$(green) TACs in the SVZ and SGZ of control and *p38α* CKO mice. Scale bars: 100 μm.

(F-I) Deletion of *p38α* induced significant reduction in the number of newborn neurons migrated from the SVZ and SGZ. Conditional deletion of *p38α* and EdU administration were performed as described in Figure 2A, followed by a 4 weeks chase and histochemical analyses. The number of $EdU^+/NeuN^+$ differentiated neurons in the olfactory bulb (OB) and dentate gyrus (DG) was significantly reduced by *p38α* deletion (*n* = 3 mice) (F and G, respectively). Representative confocal images of $NeuN^+$ (green)/EdU^+ (magenta) newborn neurons in the OB and DG of control mice and *p38α* CKO mice (H and I, respectively). Scale bars: 50 μm.

(J and K) Deletion of *p38α* did not induce significant changes in the number of apoptotic cells in the SVZ, as detected by TUNEL staining in both young (10-week-old) and aged (58-week-old) mice (*n* = 3 mice). Conditional deletion of *p38α* was induced as described in Figure 2A. Representative confocal images of TUNEL staining (green) in the SVZ of control and *p38α* CKO (10-week-old) mice (F). Scale bars: 100 μm.

(L and M) Deletion of *p38α* did not induce significant changes in the number of apoptotic cells in SGZ (*n* = 3 mice). Representative confocal images of TUNEL staining (green) in the SGZ of control and *p38α* CKO (10-week-old) mice (H). Scale bars: 100 μm. Conditional deletion of *p38α* was induced as described in Figure 2A. Nuclei were counterstained with Hoechst (blue). Statistical analysis was performed with an unpaired two-tailed Student's t-test. Values in the bar graphs represent the mean ± SD. NS: Not significant. LV: Lateral ventricle.

Figure S4. Deletion of *p38α* Does Not Alter the activation of NSCs, Related to Figure 3

(A) Representative confocal images of activated NSCs defined as $Ki67^+$ (green)/ $SOX2^+$ (magenta)/$GFAP^+$ (cyan) cells in the SVZ of control and *p38α* CKO mice (10-week-old). Scale bars: 100 μm.

(B) Deletion of *p38α* did not alter the number of $Ki67^+/SOX2^+/GFAP^+$ cells in SVZ (*n* = 6 mice).

(C) Representative confocal images of activated NSCs defined as $Ki67^+$ (green)/ $SOX2^+$ (magenta)/$GFAP^+$ (cyan) cells in SGZ of control and *p38α* CKO (10-week-old) mice. Scale bars: 100 μm.

(D) Deletion of *p38α* did not alter the number of $Ki67^+/SOX2^+/GFAP^+$ cells in the SGZ (*n* = 6 mice).

Statistical analysis was performed with an unpaired two-tailed Student's t-test.

Values in the bar graphs represent the mean ± SD. NS: Not significant. LV: Lateral ventricle.

Figure S5. Long-lasting Maintenance of NPC Proliferation and Prevention of SVZ Atrophy by Forced Expression of p38α, Related to Figure 5

(A) Representative confocal images of P-$p38^+$ (green)/$ASCL1^+$ (magenta) cells in the SVZ of 18-month-old mice. Scale bars: 50 μm.

(B) HA-immunoreactivities induced by the transgene expression were only detected by signal enhancement using TSA Plus Fluorescence kits, which was not necessary at seven days postinfection of the lentiviral vector. (Figure 5). Scale bars: 100 μm.

(C and D) p38α-overexpressing (OE) mice had a smaller ventricular area compared to control VENUS-expressing mice (*n* = 4 mice). Representative image of the lateral ventricles of mice infected with control or p38α OE lentiviruses and of mice without viral infusion (D). Scale bars: 200 μm.

(E and F) p38α OE mice had a thicker SVZ compared to control VENUS-expressing mice. The widths of dorsolateral, lateral and ventral SVZ defined by $SOX2^+$ cell layers were quantified (*n* = 3 mice). p38α OE resulted in significant increases in the thickness of dorsolateral and lateral

SVZ (E). Representative confocal images of $SOX2^+$(magenta) SVZ cell layers of control and *p38α* CKO mice (F). White lines indicate width of the lateral SVZ. Scale bars: 50 μm.

Control VENUS-expressing lentiviruses or p38α OE lentiviruses were infused into the lateral ventricles of 6-month-old mice as described in Figure 5, followed by analysis at 18 months of age. Nuclei were counterstained with Hoechst (blue or gray). Statistical analysis was performed with one-way ANOVA and the Tukey-Kramer post hoc test (C) and an unpaired two-tailed Student's t-test (E).

Values in the bar graphs represent the mean ± SD. **P* < 0.05, ***P* < 0.01. NS: not significant.

LV: Lateral ventricle. OE: Overexpression.

Figure S6. Identification of Downstream Effectors of p38, Related to Figure 6

(A) RT-qPCR analysis for 28 candidate genes known to be involved in NS/PC proliferation. Secondary neurospheres from the SVZ of 10-week-old mice were transduced with a lentiviral vector expressing shRNA targeting *p38α* mRNA (*p38* KD) or control shRNA targeting *Firefly luciferase* mRNA (sh Control) at the plating after the dissociation of primary neurospheres and were processed for RT-qPCR analyses. The heatmap represents log2-fold changes between sh Control and *p38* KD. Relative gene expression changes are depicted in color values indicated by the color key at the bottom.

(B) Differential expression of *Dkk1* and *Sfrp3* in response to *p38* KD and efficiency of *p38* KD. The relative expression of each gene is depicted as a bar graph (*n* = 3 independent cultures).

(C and D) Expression levels of *Dkk1* and *Sfrp3* mRNAs in the SGZ tissue from control, *p38α* CKO at 14-weeks (C), 12-week-old and 7-month-old wild-type mice (D) were quantified by RT-qPCR. DKK1 and SFRP3 expressions in the SGZ were significantly increased by *p38α* deficiency and with aging.

Statistical analysis was performed with an unpaired two-tailed Student's t-test.

Values in the bar graphs represent the mean ± SD. **P* < 0.05, ***P* < 0.01. KD: Knockdown.

Figure S7. Knockdown of *Dkk1* and *Sfrp3* Restores NPC Proliferation and Adult Neurogenesis, Related to Figure 6 and Figure 7

(A) Efficiencies of *Dkk1* knockdown and *Sfrp3* knockdown in neurospheres from *p38* CKO mice. Secondary neurospheres from the SVZ of 6-week-old *p38* CKO mice were transduced with a lentiviral vector expressing shRNA targeting *Dkk1* mRNA (*Dkk1* KD) or *Sfrp3* mRNA (*Sfrp3* KD) as described in Figure S6 and were processed for RT-qPCR analyses (n = 3 independent cultures).

(B) Both *Dkk1* and *Sfrp3* knockdown facilitated neurosphere growth. Neurosphere formation and lentivirus infection were performed as described above (n = 3 independent cultures).

(C) Effect of *Dkk1* and *Sfrp3* double knockdown on neurosphere growth. Neurosphere formation and lentivirus infection were performed as described above (n = 3 independent cultures).

(D) Representative confocal images of EdU^+ (magenta) and $EGFP^+$ (green) cells in 6-month-old mice SVZ transduced with *Dkk1* KD or *Sfrp3* KD lentiviral vectors. Scale bars: 100 μm.

(E and F) Both *Dkk1* and *Sfrp3* knockdown facilitated neurogenesis in the mouse SVZ. DCX^+ immature neurons (magenta) were increased by *Dkk1* KD or *Sfrp3* KD in the 6-month-old mouse SVZ (n = 3 mice). Lentiviral vectors were infused into the lateral ventricles of 6-month-old mice, and sections were processed for immunohistochemical analyses one week after injection. Scale bars: 200 μm.

Nuclei were counterstained with Hoechst (blue). Statistical analysis was performed with an unpaired two-tailed Student's t-test (A and C) or one-way ANOVA and the Tukey-Kramer post hoc test (B and E). $^*P < 0.05$, $^{**}P < 0.01$, $^{***}P < 0.001$. NS: Not significant. LV: Lateral ventricle.

Table S1, Counted SOX2^{+}/GFAP^{+} cells or ASCL1^{+} cells, related to Figure 1

Counted SOX^{+}/GFAP^{+} cells in SVZ

1 weeks	2 weeks	3 weeks	10 weeks	28 weeks	77 weeks
3124±124	1729±118	1784±82	928±34	610±18	84±12

Counted SOX2^{+}/GFAP^{+} cells in SGZ

1 weeks	2 weeks	3 weeks	10 weeks	28 weeks	77 weeks
1632±35	1416±43	756±22	374±19	262±24	10±2

Counted ASCL1^{+} cells in SVZ

1 weeks	2 weeks	3 weeks	10 weeks	28 weeks	77 weeks
844±27	693±58	613±18	351±17	133±13	16±4

Counted ASCL1^{+} cells in SGZ

1 weeks	2 weeks	3 weeks	10 weeks	28 weeks	77 weeks
975±69	781±42	151±11	111±7	4±1	1±1

Primers for quantification of mRNA of each gene			Product length
Gene		Sequence 5'-3'	
Bmi-1	Forward primer	TCTTCCTGTTTGCCCAGTCC	60
	Reverse primer	GTGAGGGAACTGTGGGTGAG	
Dkk1	Forward primer	TCTCTATGAGGGCGGGAACA	67
	Reverse primer	ATCTTCAGCGCAAGGGTAGG	
Egfr	Forward primer	ACCTTCACATCCTGCCAGTG	65
	Reverse primer	TGGGTCTAGAGGAGGAGTGC	
Ezh2	Forward primer	AGGGAGCTAAGGAGTTTGCTG	64
	Reverse primer	GGGCGTTTAGGTGGTGTCTT	
Gapdh	Forward primer	AAAGGGTCATCATCTCCGCC	65
	Reverse primer	CTCGTGGTTCACACCCATCA	
Hdac3	Forward primer	ATGTGCCGCTTCCATTCTGA	70
	Reverse primer	AACCCTGCATATTGGTGGGG	
Ilk(ILK)	Forward primer	CAAGGCACCCCTTAGAGAGC	63
	Reverse primer	CGGTTGAGATTCTGGCCCAT	
Mbd1	Forward primer	CAGCGAAGTGAGGTCAGGAG	68
	Reverse primer	GCTAGAGCTGTGGCAGTAGG	
Mbd2	Forward primer	GCTGGCAAGAGCGATGTCTA	70
	Reverse primer	TTGCCAGCTGAGGTTTACTTCT	
Mbd3	Forward primer	AGCAACAAGGTCAAGAGCGA	64
	Reverse primer	TCTCCCAGAAAAGCTGCCTC	
Mbd4	Forward primer	TGCCGAAAGGGAGCATCAAT	60
	Reverse primer	GGGAAGTCAGAGCTGCCAAA	
Mbd5	Forward primer	CAGCTTCAACCTCCCTGTCC	63
	Reverse primer	TTCCAGTCCCCATCATGTGC	
Mbd6	Forward primer	TATCAGCCCAAGTGGCACAG	60
	Reverse primer	CTGAGGAGGTAGCTACGGGT	
mcbp2	Forward primer	CACCACTACCACAGTTGCAGA	61
	Reverse primer	AATGTCTTTGCGCTCTCCCT	
Nampt	Forward primer	AGGGGCATCTGCTCATTTGG	61
	Reverse primer	TAGAGCAATTCCCGCCACAG	
Nrf1	Forward primer	CATGGGCGGGAGGATCTTTT	61
	Reverse primer	TGGTGGCCTGAGTTTGTGTT	
Nrf2	Forward primer	AAGAATAAAGTCGCCGCCCA	62
	Reverse primer	TCCAGCTCGACAATGTTCTCC	
p15	Forward primer	AGGTCATGATGATGGGCAGC	66
	Reverse primer	AGTTGGGTTCTGCTCCGTG	
p16	Forward primer	CGTAGCAGCTCTTCTGCTCA	64
	Reverse primer	GGAGAAGGTAGTGGGGTCCT	
p18	Forward primer	GAACTGCGCTGCAGGTTATG	62
	Reverse primer	TCTGAGGAGAAGCCTCCTGG	
p19	Forward primer	TAGTCCTGTGCATGATGCGG	66
	Reverse primer	CCATGCTCCACCAGAACCTT	
p21	Forward primer	TTGCACTCTGGTGTCTGAGC	70
	Reverse primer	TTTCGGCCCTGAGATGTTCC	
p38	Forward primer	GATGTGTTCACACCCGCAAG	61
	Reverse primer	GATGGGTCACCAGGTACACG	
p53	Forward primer	CCATGGCCCCTGTCATCTTT	60
	Reverse primer	GAAGCCATAGTTGCCCTGGT	
p57	Forward primer	TTCCCAGTGATAGCGCGTAG	66
	Reverse primer	CAGCTCCTCGTGGTCTACAG	
Pax6	Forward primer	GAGTAAGCCAAGAGTGGCGA	70
	Reverse primer	GGAAGGGCACTCCCGTTTAT	
Pgc1	Forward primer	CACGTTCAAGGTCACCCTACA	69
	Reverse primer	GCCTTTCGTGCTCATAGGCT	
Sfrp3	Forward primer	ACCCATTTGCACCATCGACT	60
	Reverse primer	TCACACACAGACTTGCAGGG	
Tfam	Forward primer	ACACCCAGATGCAAAACTTTCAG	67
	Reverse primer	TTCTGGTAGCTCCCTCCACA	
Yap1	Forward primer	GCATGTTCGAGCTCACTCCT	64
	Reverse primer	GAGTGTCCCAGGAGAAACGG	

Table S2, Primers for quantification of mRNA of each gene

Supplemental Experimental Procedures

Neurosphere culture

The adult SVZ tissues dissected from wild-type or *p38α* CKO mice were dissociated into single cells after incubation in TrypLE™ Select (Thermo Fisher Scientific, 12563029) with DNase I (Worthington Biochemical, LS002138) for 10 min at 37 °C. Dissociated cells were plated at a density of 1×10^5 cells/mL in a growth medium composed of D-MEM/Ham's F-12 (Wako, 042-30795), 20 ng/mL bFGF (PeproTech, 100-18B), 20 ng/mL EGF (PeproTech, AF-100-15), 2 % B27 supplement (Thermo Fisher Scientific, 7504-044), 1 % penicillin/streptomycin (Nacalai Tesque, 26253-84), 20 ng/mL IGF-I (BioLegend, 590996), and 0.02 % heparan sulfate (Sigma-Aldrich, H7640-1MG) into 6-Well Clear Flat Bottom Ultra Low Attachment Multiple Well Plates (Corning, 3471) and cultured for 10 days to form primary neurospheres. The primary neurospheres were then mechanically dissociated and plated at a density of 1×10^5 cells /mL in the growth medium and cultured for six days to form secondary neurospheres.

Analysis of proliferation in neurospheres

To assess the proliferation index of NS/PCs derived from adult SVZs in vitro, neurospheres were plated on poly-L-ornithine/fibronectin-coated chamber slide glasses (IWAKI, 5732-008), incubated for 30 min, and then exposed to EdU (10 μM) for another 30 min at 37 ℃, followed by fixation in 4 % paraformaldehyde (PFA)/phosphate buffered saline (PBS) for 30 min. To detect incorporated EdU (Invitrogen, E10187), we used a Click-iT™ Plus EdU Alexa Fluor™ 555 Imaging Kit (Thermo Fisher Scientific, C10638) following the manufacturer's instructions. At least 3 independent trials were conducted in all experiments. More than 500 cells per individual cultures were quantified.

We analyzed these samples with a confocal laser scanning microscope LSM700 (Carl Zeiss) or an All-In-One Fluorescence Microscope BZ-X700 (Keyence).

Lentivirus production

Lentiviruses were produced by transient transfection of Lenti-X 293T cells (Takara Bio, Inc., 632180) with the lentivirus constructs, pCMV-VSV-G-RSV-Rev and pCAG-HIVgp48 using GeneJuice® Transfection Reagent (Merck Millipore, 70967-6CN) according to the manufacturer's instructions. High-titer (>10^9 IFU/mL) concentrated stocks prepared by ultracentrifugation and resuspension in PBS were used to obtain efficient infections.

Lentiviral infection

Secondary neurospheres derived from adult mouse SVZs at various ages were transduced with lentiviral vectors expressing VENUS or *p38α* tagged with a 3xHA sequence under the control of the human EF1 promoter (Naka-Kaneda et al., 2014) (MOI = 3), small hairpin RNA targeting *Firefly luciferase* (control), *p38α* (Naka-Kaneda et al., 2014), *Dkk1,* or *Sfrp3* (*Dkk1* shRNA sequence: 5'-GGGAAATTGAGGAAAGCAT-3'; *Sfrp3* shRNA sequence: 5'-GCGAGCCCATTCTCATCAA-3') under the control of the human H1 promoter with the EGFP reporter driven by the human EF-1 promoter (Naka et al., 2008) (MOI = 20) at the plating after the dissociation of primary neurospheres.

To transduce the lentiviruses into SVZ cells in vivo, a cannula (PlasticsOne, C315GS- 4/SPC, C315DCS- 4/SPC, C315IS- 4/SPC) was installed into the right lateral ventricle. To avoid the effect of the inflammatory response, the virus administration was carried out (10^{10} IFU/mL, 2 μL) one week after the construction of the cannula in the mouse brain. Infected mice were injected with EdU (50 mg/kg) two hours before the sacrifice for histological analysis at 7 days postinfection.

Immunostaining

For immunohistochemistry, vibratome sections were prepared by standard protocols after perfusion and fixation with 4 % PFA/PBS. The sections were treated with 3 % H_2O_2 /PBS for 10 min to quench endogenous peroxidase activity and then processed for antigen retrieval optimized for each antibody as described below. Subsequently, the sections were permeabilized in 0.3 % Triton -X100 (Sigma-Aldrich, X100-1GA)/PBS for 30 min at room temperature. After blocking in TNB buffer (0.1 M Tris-HCl, pH 7.5, 0.15 M NaCl, 0.5 % [w/v] blocking reagent [PerkinElmer, FP1020]) for 1 h at room temperature, the sections were incubated at 4 °C overnight with the following antibodies: rabbit monoclonal anti-p38 MAPK (Cell Signaling Technology, 8690L; 1:500), rabbit monoclonal anti-phospho-p38 MAPK (Cell Signaling Technology, 4511L; 1:500), goat polyclonal anti-Doublecortin (Santa Cruz Biotechnology, sc-8066; 1:500), mouse monoclonal anti-MASH1(ASCL1) (BD PharMingen, 556604; 1:200), goat polyclonal anti-SOX2 (Abcam, ab110145; 1:500), rat monoclonal anti-GFAP (Invitrogen, 13-0300; 1:500), mouse monoclonal anti-Ki67 (Leica Biosystems, PA0118; 1:50), rat monoclonal anti-HA (Sigma-Aldrich, 12158167001; 1:250), rabbit monoclonal non-phospho (active) β-Catenin antibody, clone D13A1 (Cell Signaling Technology, 8814; 1:500). Antigen retrieval was accomplished by incubation at 80 ℃ for 30 min in 10 mM sodium citrate buffer for anti-p38 MAPK, anti-phospho-p38 MAPK or in 1 N HCl for 30 min for anti-MASH1, anti-non-phospho β-Catenin antibody at room temperature. After washing with PBS three times, the sections were incubated for 90 min at room temperature with secondary antibodies conjugated with Alexa 488 (Thermo Fisher Scientific, A-11034 or A-11001 or A-11055; 1:500) or Alexa 555 (Thermo Fisher Scientific, A-21429 or A-21434 or A-21422 or A-21432; 1:500) or Alexa 647 (Thermo Fisher Scientific, A-21247; 1:500). For anti-p38 MAPK, anti-phospho-p38 MAPK, anti-MASHI1, anti-Ki67, anti-HA, and anti-non-phospho β-Catenin staining, we used biotinylated secondary antibodies (Jackson ImmunoResearch, 111-065-144 or 712-065-153 or 115-065-146; 1:500).

The signals were then enhanced with a VECTASTAIN Elite ABC HRP Kit (Vector Laboratories, PK-6100), followed by a TSA™ Fluorescein System (Perkin Elmer, NEL701001KT or NEL702001KT) or TSA Plus Fluorescein / TMR System (Perkin Elmer, NEL756001KT). Cell nuclei of the sections were counterstained with Hoechst 33258 (Sigma-Aldrich, B2883; 10 μg/mL). The sections were mounted on glass slides and analyzed with a confocal laser scanning microscope LSM700 (Carl Zeiss). We counted all labeled cells in each section containing whole SVZ or DG of a cerebral hemisphere and compared the number at the same brain coordinate. For counting labeled cells in olfactory bulb, we counted the number of cells per mm^2 of arbitrary area in the granule cell layer.

For immunocytochemistry, neurospheres were plated onto poly-L-ornithine/fibronectin-coated chamber slide glasses (IWAKI, 5732-008) and fixed in 4 % PFA/PBS for 30 min at room temperature. The slides were rinsed with PBS three times, followed by cell permeabilization in 0.3 % Triton -X100/PBS for 5 min at room temperature. After blocking in TNB buffer for 15 min at room temperature, the slides were incubated at 4 °C overnight with the following antibodies: rabbit monoclonal anti-p38 MAPK (Cell Signaling Technology, 8690L; 1:500), rabbit monoclonal anti-phospho-p38 MAPK (Cell Signaling Technology, 4511L; 1:500), rabbit monoclonal anti-p38α MAPK (Cell Signaling Technology, 9218L; 1:500), rat monoclonal anti-Nestin (BD PharMingen, 556309; 1:500), rat monoclonal anti-HA (Sigma-Aldrich, 12158167001; 1:500). After washing with PBS three times, the neurospheres were incubated for 60 min at room temperature with secondary antibodies conjugated with Alexa 488 (Thermo Fisher Scientific, A-11034 or A-11001) or Alexa 555 (Thermo Fisher Scientific, A-21429 or A-21434), followed by nuclear counterstaining with Hoechst 33258 (Sigma-Aldrich, B2883; 10 μg/mL), and we analyzed these samples with a confocal laser scanning microscope LSM700 (Carl Zeiss) or an All-In-One Fluorescence Microscope BZ-X700 (Keyence).

Quantitative reverse-transcription PCR

Total RNA of each sample was isolated by using an RNeasy Mini Kit (250) (Qiagen, 74106). Complementary DNA was reverse transcribed using SuperScript™ IV Reverse Transcriptase (Invitrogen, 18090050). qPCR was performed by using SYBR® Premix Ex Taq™ II (Takara Bio, Inc., RR820A) and a ViiA 7 Real-Time PCR System (Thermo Fisher Scientific) according to the manufacturer's protocol. Fold changes were calculated using the ΔΔCt comparative quantification method. For the primer sequences, see Table S1. Expression levels of all genes of interest were normalized to *Gapdh* mRNA levels.

Western blot analysis

Rabbit monoclonal non-phospho (active) β-Catenin antibody, clone D13A1 (Cell Signaling Technology, 8814; 1:500), anti-β-ACTIN antibody (Sigma-Aldrich, A1978-100UL; 1:500) were used as primary antibodies, and anti-rabbit IgG antibody (HRP-conjugated) (Jackson ImmunoResearch, 111-035-144; 1:3000), anti-mouse IgG antibody (HRP-conjugated) (Jackson ImmunoResearch, 115-035-166; 1:3000) were used as the secondary antibody. Neurospheres from each condition were lysed in lysis buffer (Sigma) with Halt™ Phosphatase Inhibitor Cocktail (Thermo Fisher Scientific, 78420). Loading samples were prepared and separated by SDS-PAGE (4-15 %) and processed for Western blotting with a standard protocol. Signals were detected using ECL Prime Western blotting Detection Reagent (GE Healthcare, RPN2236) and visualized using a LAS-4000mini luminescent image analyzer (Fujifilm). For quantification, we used the inbuilt function for ‘‘Gels’’ to first convert band intensities into histograms, from which the area under the curve could be measured using the Wand tool, and the relative expression between control and treated samples were calculated using ImageJ software (NIH).

Apoptosis assay

Apoptotic cells in the brain sections were detected using an In Situ Cell Death Detection Kit, Fluorescein (Sigma-Aldrich, 11684795910) following the manufacturer's protocol.

SA-β-GAL assay

SA-β-gal activity was detected by using a 96-well Cellular Senescence Assay Kit (Cell Biolabs, Inc., CBA-231), and the intensity of SA-βgal activity was quantified using a fluorescence plate reader, Cytation 5 (BioTek). To visualize SA-βgal activity, neurospheres were fixed and processed for SA-β-gal staining using a Senescence Detection Kit (BioVision, K320-250).

Supplemental References

Naka, H., Nakamura, S., Shimazaki, T., and Okano, H. (2008). Requirement for COUP-TFI and II in the temporal specification of neural stem cells in CNS development. Nat. Neurosci. *11*, 1014–1023.